Supporting Information

Solomon *et al.* **10.1073/pnas.0812721106**

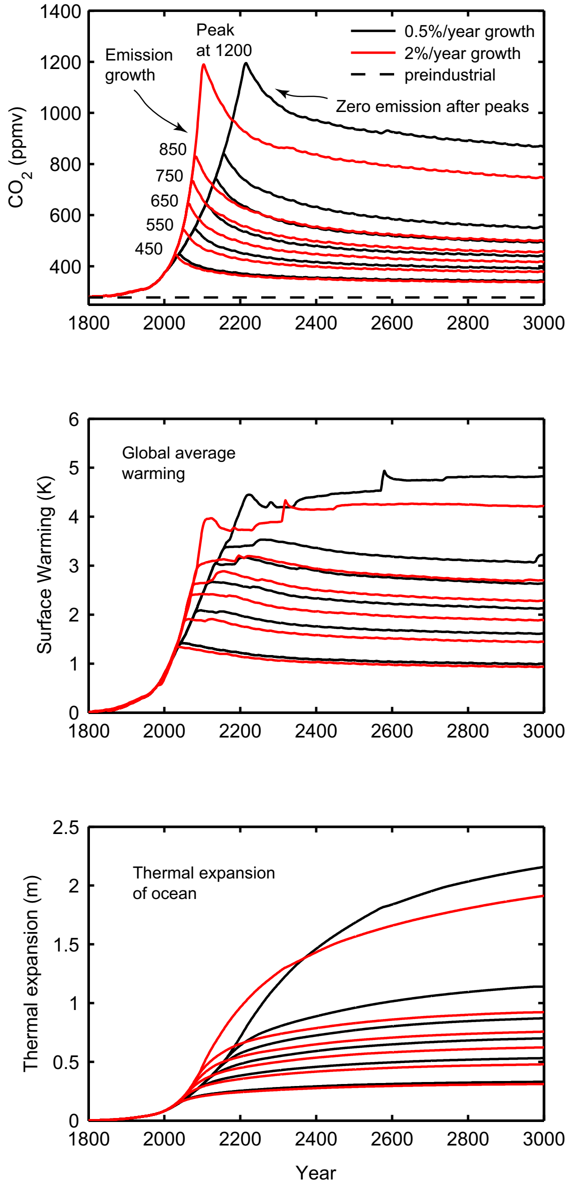

Fig. S1. Carbon dioxide and climate system changes (relative to preindustrial conditions in 1765) from 1 illustrative model, the Bern 2.5CC EMIC, whose results are comparable to the suite of assessed EMICs (1, 2) (see Fig. 1). (*Top*) Falloff of CO_2 concentrations following zero emissions, from peak values of 450, 550, 650, 750, 850, and 1200 ppmv. Black and red lines depict 2 different illustrative future rates of emission growth of 0.5%/year and 2%/year before reaching these peak levels. Total emissions in the 0.5%/year cases are higher than in the corresponding 2%/year cases as the peak CO_2 levels are reached later on, which results in larger climate changes for large perturbations (3). (*Middle*) Globally averaged surface warming (degrees Celsius) for these cases (note that this model has an equilibrium climate sensitivity of 3.2 °C for carbon dioxide doubling). (*Bottom*) Sea level rise (meters) from thermal expansion only (not including glaciers, ice caps, or ice sheets).

1. Meehl GA, *et al.* (2007) in *Climate Change 2007: The Physical Science Basis*, eds Solomon S, *et al.* (Cambridge Univ Press, Cambridge, UK), pp 747–845.
2. Plattner GK, *et al.* (2008). Long-term climate commitments projected with climate-carbon cycle models. *J Clim* 21:2721–2751.
3. Eby M, *et al.* (2008) Lifetime of anthropogenic climate change: Millennial time-scales of potential CO_2 and surface temperature perturbations *J Clim*, in press.

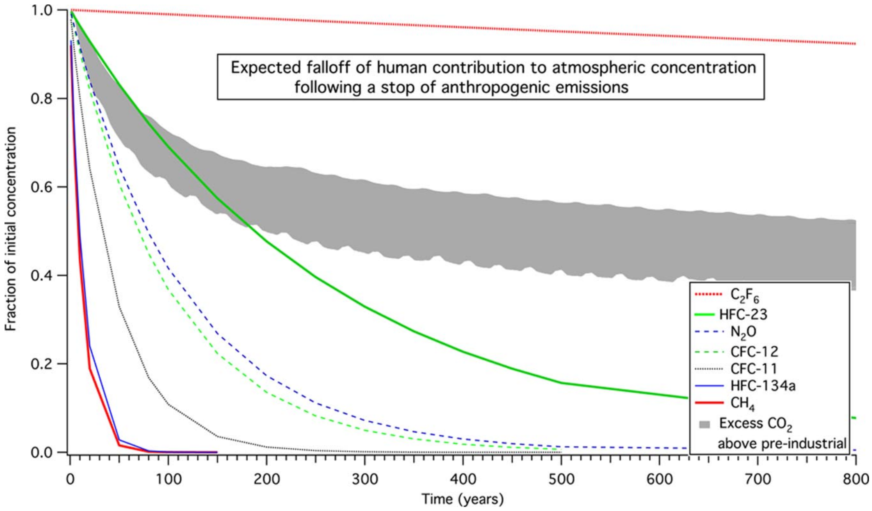

Fig. S2. Typical falloff of concentrations expected for various greenhouse gases, from a peak value following cessation of emissions. The decay of CH_4, N_2O, and halocarbons depends upon their atmospheric lifetimes, which are well represented for realistic cases as single values and are taken from ref. 1. The range of CO_2 decay is based upon calculations with the Bern2.5CC carbon cycle–climate model for the 2%/year rate of increase cases shown in Fig. 1 of the main text covering a broad range of cases in which CO_2 concentrations increase from current concentrations to peak values of 450-1200 ppmv and then emissions are halted. The 31-year variation seen in the carbon dioxide decay is introduced by the climatology used to force the terrestrial biosphere model (2).

1. Forster P, *et al.* (2007) Changes in atmospheric constituents and in radiative forcing. *Climate Change 2007: The Physical Science Basis*, eds Solomon S, *et al.*(Cambridge Univ Press, Cambridge, UK), pp 747–845.
2. Joos F, *et al.* (2001) Global warming feedbacks on terrestrial carbon uptake under the Intergovernmental Panel on Climate Change (IPCC) emission scenarios. *Global Biogeochem Cycles* 15:891–907.

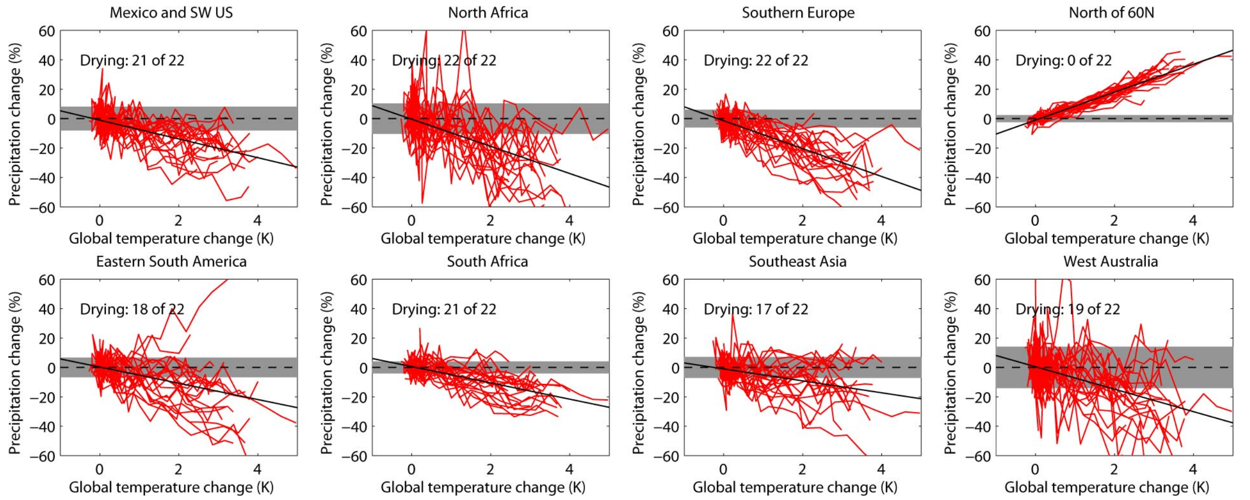

Fig. S3. Relationship between temperature and rainfall averaged over several large regions for a suite of 22 AOGCMs (1, 2) relative to the baseline period of 1900–1950. Two available outlying models that differ greatly from all other AOGCMs were not included, but this choice does not materially affect the results because there are so many models. The model outputs are available at www-pcmdi.llnl.gov/ipcc/about_ipcc.php. Data have been averaged over the regions shown in Fig. 3 (main text) and over a decade, for the 3 driest consecutive months in the baseline period. One ensemble member is used for each model so that all models are equally weighted in a multimodel ensemble. The gray shaded area delimits 1 standard deviation among the models during the baseline period from 1900 to 1950 to estimate the likely uncertainty. The number of models showing drying in each region is indicated.

1. Meehl GA, *et al.* (2007) Global climate projections. *Climate Change 2007: The Physical Science Basis*, eds Solomon S, *et al.* (Cambridge Univ Press, Cambridge, UK and New York), pp 747–845.
2. Meehl GA, *et al.* (2007) The WCRP CMIP3 multi-model dataset: a new era in climate change research. *Bull Am Meteorol Soc* 88:1383–1394.

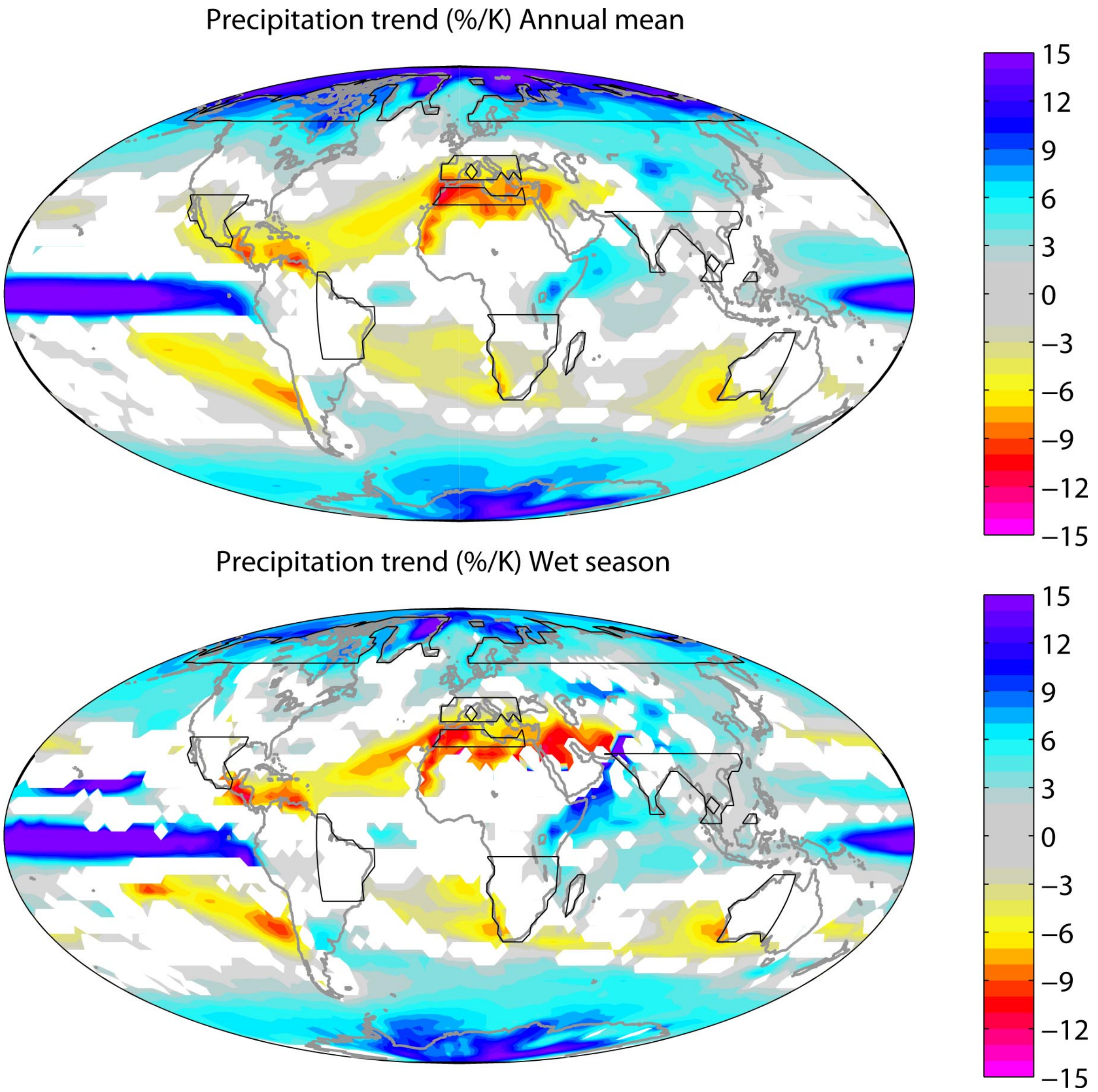

Fig. S4. The same as in Fig. 3 of the main text, but for the annual mean and for the 3 consecutive wettest months. Decadally averaged changes in the global distribution of precipitation per degree of warming are shown (percentage of change in precipitation per degree of warming, relative to 1900–1950 as the baseline period) at each grid point, on the basis of a suite of 22 AOGCMs. White is used where <16 of 22 models agree on the sign of the response, while colors and gray indicate grid points where at least 16 of the 22 models agree.